EFFECTS OF TIME DELAY ON THE DYNAMICS OF A KINETIC MODEL OF A MICROBIAL FERMENTATION PROCESS

KASBAWATI[1,3], A. Y. GUNAWAN[✉1], R. HERTADI[2] and K. A. SIDARTO[1]

Abstract

We examine the dynamics of fermentation process in a yeast cell. Our investigation focuses on the main branch pathway: pyruvate and acetaldehyde branch points. We formulate the kinetics for all enzymatic reactions as Michaelis–Menten models. Since the activity of an enzyme mainly depends on the conformational changes of the enzyme structure, the enzyme requires a certain period of time to reset its structure, until it is ready to bind substrates again. For this situation, a rate-limiting step exists, for which the catalytic process suffers a delay. Since all conversion processes are catalysed by enzymes, each reaction can experience a delay at a different time. To investigate how the delay affects the reaction processes, especially at the branch points, we propose that the rate-limiting step takes place at the first reaction. For this reason, a discrete time delay is introduced to the first kinetic model. We find a bifurcation diagram for the delay that depends on the rate of glucose supply and kinetic parameters of the first enzyme. By comparison, our analysis agrees with the numerical solution. Our numerical simulations also show that there is a certain glucose supply that may optimize ethanol production.

2010 *Mathematics subject classification*: primary 92C45; secondary 34K60, 34K99.

Keywords and phrases: fermentation process, single enzyme–substrate reaction mechanism, enzyme kinetic, time delay, Hopf bifurcation.

1. Introduction

Metabolism is a highly regulated chemical reaction involving many enzymes, which cooperate to transform nutrient molecules into the cell's own characteristic molecules.

[1]Industrial and Financial Mathematics Research Group, Faculty of Mathematics and Natural Sciences, Institut Teknologi Bandung, Jl. Ganesha 10, Bandung, Indonesia; e-mail: aygunawan@math.itb.ac.id, sidarto@math.itb.ac.id.
[2]Biochemistry Research Division, Faculty of Mathematics and Natural Sciences, Institut Teknologi Bandung, Jl. Ganesha 10, Bandung, Indonesia; e-mail: rukman@chem.itb.ac.id.
[3]Department of Mathematics, Faculty of Mathematics and Natural Sciences, Hasanuddin University, Jl. Perintis Kemerdekaan Km. 10, Makassar, Indonesia; e-mail: kasbawati@gmail.com.

The system consists of thousands of interconnected chemical reactions catalysed by different enzymes which have well-defined molecular structures and involves the measurement of the kinetic parameters, such as maximum enzyme activity, substrate binding, and inhibition constant. Any change in the kinetic properties of the enzyme influences the survival and functional performance of a metabolic system. Theoretical studies on the problem of designing the kinetic properties of enzymes to produce optimal performance have been developed mostly to overcome various industrial problems [7, 11–13, 15]. These studies aim to determine possible strategies for controlling or manipulating the metabolic processes.

Kinetic modelling has been widely used to integrate and elaborate the properties of a metabolic system. Many structured kinetic models have been developed to describe the metabolic state of the cell in stationary and time-dependent states, particularly in a normal physiological condition, i.e. when the enzyme activity is not disturbed [2, 5, 14, 19, 30]. However, the change in the activity of an enzyme certainly affects the metabolic process. One of the possible causes is the existence of the rate-limiting step in the conversion process. From the experiments, it was reported that the enzyme activity mainly depends on the conformational changes of the enzyme structure, which take place from the moment an enzyme complex is formed until the product is released [1, 3, 4, 9, 16]. Consequently, the enzyme requires a certain time to reset its structure until it is ready to bind the substrate again. The interesting question is how we elucidate the structure completion process in terms of a delay process and how this affects the whole catalytic process. In the present work, we study a kinetic model which takes into account the effect of delay on the substrate conversion. We focus on the main pathway of a yeast cell: the pyruvate and acetaldehyde branch points as shown in Figure 1. Our mathematical model is based on the Michaelis–Menten kinetic model with discreet time delay, which is likely to play an important role in causing oscillatory behaviour.

The paper is organized as follows. In Section 2 we describe the formulation of a kinetic model of the fermentation pathway with delay effect. In Section 3 we investigate the stability of the delay differential system. In Section 4 we show the numerical simulations and compare our theoretical results with these simulations. A summary and some concluding remarks are presented in Section 5.

2. Formulation of kinetic model with delay effect

In this section we derive a mathematical model to describe the dynamics of the branched metabolic pathway in a yeast cell. The pathway is a series of enzyme-catalysed reactions which convert substrate molecules to other molecules and generate final metabolites. This work follows along the lines of Lei et al. [19], but for a different pathway (see Figure 1). The model is based on the following assumptions.
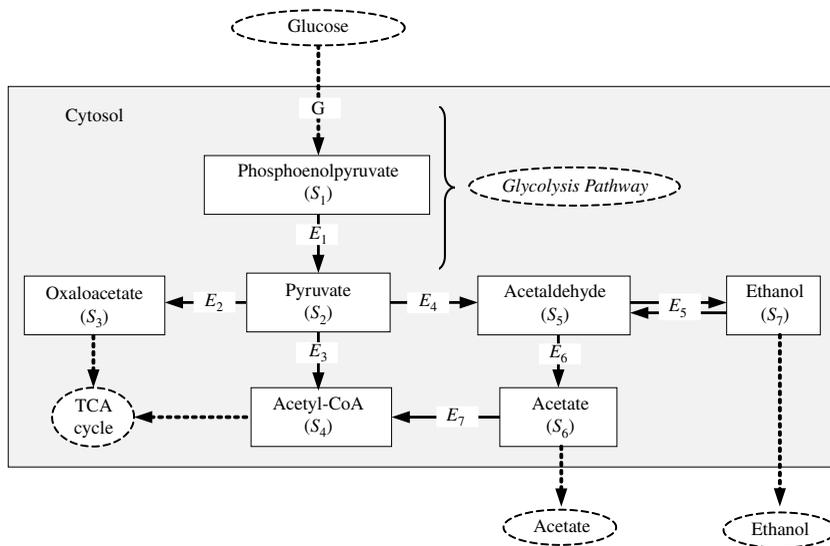
FIGURE 1. Schematic representation of enzymatic reactions at the pyruvate and acetaldehyde branch points in *Saccharomyces cerevisiae*. The symbol G refers to the rate of glucose supply. All reactions are catalysed by the following enzymes: E_1 = pyruvate kinase, E_2 = pyruvate carboxylase, E_3 = pyruvate dehydrogenase complex, E_4 = pyruvate decarboxylase, E_5 = alcohol dehydrogenase, E_6 = acetaldehyde dehydrogenase, E_7 = acetyl-CoA synthetase. The TCA cycle is the tricarboxylic acid cycle [24].

(1) The model describes the anaerobic growth of a yeast cell under ideal fermentation conditions. The uptake of glucose (G) is assumed to be constant per unit time, and it is metabolized via the glycolysis pathway to produce substrate S_1. Then enzyme E_1 catalyses the first reaction to produce substrate S_2 which is the last product of the glycolysis pathway. In the present work we shall focus on the investigation of the enzymatic reaction process inside a single yeast cell. We do not include the product inhibition effects on the growth of the yeast cell. This feature will be considered in a later paper.

(2) The first overflow metabolism occurs at the first branch, where the substrate S_2 is converted into three intermediate substrates, S_3, S_4, S_5, through catalysis of the three different enzymes. Substrates S_3 and S_4 are then used in the tricarboxylic acid (TCA) cycle which is a series of enzyme-catalysed chemical reactions that become a key part of the aerobic respiration in the yeast cell, and substrate S_5 is preferably converted to acetate by enzyme E_6. However, saturation of enzyme E_5 leads to ethanol production. Moreover, through catalysis of enzyme E_7, substrate S_6 is converted into S_4, which will end in the TCA cycle as well.

(3) The modelling of all reaction rates is based on Michaelis–Menten kinetic models. Due to the properties of all enzymes, all reactions are irreversible except for the fifth reaction [22, 24]. The rate equation for the irreversible

reactions is

$$u_i(t) = \frac{V_i S_i(t)}{S_i(t) + K_i}, \quad i = 1, \ldots, 4, 6, 7, \tag{2.1}$$

and for the reversible reaction it is

$$u_5(t) = \frac{V_5^f K_5^b S_5(t) - V_5^b K_5^f S_7(t)}{K_5^f K_5^b + K_5^b S_5(t) + K_5^f S_7(t)}. \tag{2.2}$$

The derivation of (2.2) is given in the Appendix. Equations (2.1) and (2.2) are single enzyme–substrate reaction rates which refer to the reaction rates catalysed by enzyme i with maximum reaction rate V_i for $i = 1, \ldots, 7$ and Michaelis constant K_i. Note that indices f and b in (2.2) refer to the forward and backward direction in the reversible reaction, respectively (see [18]). In this work, we do not model the equations for the enzyme species since we focus on the dynamics of the substrates and the products only.

(4) The activity of an enzyme mainly depends on the conformational changes in the enzyme structure [1, 3, 4, 9, 16]. The enzyme structure change takes place from the moment an enzyme complex is formed until a product is released. It is based on the fact that when an enzyme catalyses a reaction, its structure changes due to the binding of a substrate to an enzyme at the active site [22]. Consequently, the enzyme requires a completion time to reset its structure before it is ready to bind a substrate again [1, 4, 9]. Thus, there is a rate-limiting step in reaction which induces a delay from the moment an enzyme–substrate complex is formed until a product molecule is released. Hence, a recovery time is needed to reset the conformational change of the enzyme [17, 27]. Since all conversion processes are catalysed by enzymes, each reaction can experience a delay at a different time. In the absence of specific knowledge or experimental evidence any given step is a rate-limiting step in the fermentation pathway, we assume that the rate-limiting takes place at the first reaction. Indeed, when the first reaction suffers a delay, the other reactions are also affected by this delay. To investigate how the delay affects the fermentation reaction process, we introduce a single discreet time delay in the first kinetic,

$$u_1(t - \tau) = \frac{V_1 S_1(t - \tau)}{S_1(t - \tau) + K_1}, \quad \tau > 0,$$

where $S_1(t - \tau)$ is defined as the concentration of the first metabolite when delay occurs for time τ, where τ is the length of time required by E_1 to convert S_1 into S_2. Using the mass action rate law [18], we derive the delay differential

equations as follows:

$$\text{(a)} \quad \frac{dS_1(t)}{dt} = G - u_1(t - \tau),$$

$$\text{(b)} \quad \frac{dS_2(t)}{dt} = u_1(t - \tau) - u_2(t) - u_3(t) - u_4(t),$$

$$\text{(c)} \quad \frac{dS_3(t)}{dt} = u_2(t) - \delta_1 S_3(t),$$

$$\text{(d)} \quad \frac{dS_4(t)}{dt} = u_3(t) + u_7(t) - \delta_2 S_4(t), \tag{2.3}$$

$$\text{(e)} \quad \frac{dS_5(t)}{dt} = u_4(t) - u_5(t) - u_6(t),$$

$$\text{(f)} \quad \frac{dS_6(t)}{dt} = u_6(t) - u_7(t) - \delta_3 S_6(t),$$

$$\text{(g)} \quad \frac{dS_7(t)}{dt} = u_5(t) - \delta_4 S_7(t).$$

The conditions imposed on the problem are $S_1(t) = S_1^0$ (a constant) for $[-\tau, 0]$ and $S_i(0) = 0$ for $i > 1$. Outflows in (2.3)(c, d, f, g) are assumed to be linear functions of S_i, where δ_i is a constant for $i = 3, 4, 6, 7$. All parameters are assumed to be positive. Furthermore, the maximum rate of inflow should be less than the maximum rate of outflow in every stage, e.g. at the first stage $G < V_1$, at the first branch point, $V_1 < V_i$, $i = 2, 3, 4$, and at the second branch point $V_4 < V_6 < (V_6 + V_5^f)$. These physical intuitions will be confirmed in Section 3. Rescaling all variables via $S_i = K_1 x_i$ and time scale $t = \tau \tilde{t}$, we get the dimensionless system,

$$\text{(a)} \quad \frac{dx_1(\tilde{t})}{d\tilde{t}} = \tilde{G} - \frac{v_1 x_1(\tilde{t} - 1)}{x_1(\tilde{t} - 1) + 1},$$

$$\text{(b)} \quad \frac{dx_2(\tilde{t})}{d\tilde{t}} = \frac{v_1 x_1(\tilde{t} - 1)}{x_1(\tilde{t} - 1) + 1} - \frac{v_2 x_2(\tilde{t})}{x_2(\tilde{t}) + \kappa_2} - \frac{v_3 x_2(\tilde{t})}{x_2(\tilde{t}) + \kappa_3} - \frac{v_4 x_2(\tilde{t})}{x_2(\tilde{t}) + \kappa_4},$$

$$\text{(c)} \quad \frac{dx_3(\tilde{t})}{d\tilde{t}} = \frac{v_2 x_2(\tilde{t})}{x_2(\tilde{t}) + \kappa_2} - \sigma_1 x_3(\tilde{t}),$$

$$\text{(d)} \quad \frac{dx_4(\tilde{t})}{d\tilde{t}} = \frac{v_3 x_2(\tilde{t})}{x_2(\tilde{t}) + \kappa_3} + \frac{v_7 x_6(\tilde{t},)}{x_6(\tilde{t},) + \kappa_7} - \sigma_2 x_4(\tilde{t}), \tag{2.4}$$

$$\text{(e)} \quad \frac{dx_5(\tilde{t})}{d\tilde{t}} = \frac{v_4 x_2(\tilde{t})}{x_2(\tilde{t}) + \kappa_4} - \frac{v_{5f}\kappa_{5b} x_5(\tilde{t}) - v_{5b}\kappa_{5f} x_7(\tilde{t})}{\kappa_{5f}\kappa_{5b} + \kappa_{5b} x_5(\tilde{t}) + \kappa_{5f} x_7(\tilde{t})} - \frac{v_6 x_5(\tilde{t})}{x_5(\tilde{t}) + \kappa_6},$$

$$\text{(f)} \quad \frac{dx_6(\tilde{t},)}{dt} = \frac{v_6 x_5(\tilde{t})}{x_5(\tilde{t}) + \kappa_6} - \frac{v_7 x_6(\tilde{t},)}{x_6(\tilde{t},) + \kappa_7} - \sigma_3 x_6(\tilde{t},),$$

$$\text{(g)} \quad \frac{dx_7(\tilde{t})}{d\tilde{t}} = \frac{v_{5f}\kappa_{5b} x_5(\tilde{t}) - v_{5b}\kappa_{5f} x_7(\tilde{t})}{\kappa_{5f}\kappa_{5b} + \kappa_{5b} x_5(\tilde{t}) + \kappa_{5f} x_7(\tilde{t})} - \sigma_4, x_7(\tilde{t}),$$

where the dimensionless parameters are given by

$$\tilde{G} = \frac{\tau G}{K_1}, \quad \nu_j = \frac{V_j \tau}{K_1}, \quad \kappa_j = \frac{K_j}{K_1}, \quad \kappa_{5f} = \frac{K_1}{K_5^f}, \quad \kappa_{5b} = \frac{K_1}{K_5^b}, \quad \sigma_i = \delta_i \tau$$

for $i = 1, \ldots, 4$ and $j = 1, \ldots, 7$.

3. Stability analysis

In this section, we analyse the steady-state solution of system (2.4) defined in the restriction region,

$$\mathbb{R}_+^7 = \{(x_1, x_2, x_3, x_4, x_5, x_6, x_7) \in \mathbb{R}^7 \mid x_i \geq 0, i = 1, \ldots, 7\}.$$

Equation (2.4) is defined in the region $\mathbb{R}_+^7$, because the vector field on the boundary of $\mathbb{R}_+^7$ does not point to the exterior of $\mathbb{R}_+^7$. Furthermore, the equilibria of system (2.4) can be determined by setting $\dot{x}_i = 0$, for $i = 1, \ldots, 7$. Fixing the right-hand side of (2.4)(a) to zero gives $x_1^* = \tilde{G}/(\nu_1 - \tilde{G})$. This is in $\mathbb{R}_+^7$ as long as $\nu_1 > \tilde{G}$. This condition guarantees the existence of the equilibrium solution of the first substrate, and it directly confirms our physical assumption made earlier. For equation (2.4)(b), with $x_1^* = \tilde{G}/(\nu_1 - \tilde{G})$, we find a cubic equation,

$$a_1(x_2)^3 + a_2(x_2)^2 + a_3 x_2 + a_4 = 0, \tag{3.1}$$

with

$$
\begin{aligned}
a_1 &= (\nu_2 + \nu_3 + \nu_4) - \tilde{G}, \\
a_2 &= (\nu_3 + \nu_4 - \tilde{G})\kappa_2 + (\nu_4 + \nu_2 - \tilde{G})\kappa_3 + (\nu_2 + \nu_3 - \tilde{G})\kappa_4, \\
a_3 &= (\nu_2 - \tilde{G})\kappa_3\kappa_4 + (\nu_3 - \tilde{G})\kappa_2\kappa_4 + (\nu_4 - \tilde{G})\kappa_2\kappa_3, \\
a_4 &= -\tilde{G}\kappa_2\kappa_3\kappa_4.
\end{aligned}
$$

If $\nu_i > \tilde{G}$ for $i = 2, 3, 4$, then coefficient a_3 is positive, as well as a_1 and a_2. Using Descartes' rule of signs [21], we observe that equation (3.1) has only one positive root since there is only one turnover sign on its coefficients. Thus from (3.1), we obtain only one positive equilibrium solution. Since the first reaction is rate-limiting, we have conditions, i.e. $\tilde{G} < \nu_1 < \nu_i$, $i = 2, 3, 4$, that make x_1^* and x_2^* positive. Furthermore, equations (2.4)(c, d) have equilibrium solutions,

$$x_3^* = \frac{\nu_2 x_2^*}{(x_2^* + \kappa_2)\sigma_1} \quad \text{and} \quad x_4^* = \frac{1}{\sigma_2}\left[\frac{\nu_3 x_2^*}{(x_2^* + \kappa_3)} + \frac{\nu_7 x_6^*}{(x_6^* + \kappa_7)}\right],$$

which depend on x_2^* and x_6^*. Note that x_6^* is a root of (2.4)(f) which will be analysed below (see equation (3.5)). Now, from equations (2.4)(e, g), we have

$$
\begin{aligned}
\text{(a)} \quad &\xi_1 - \frac{\nu_{5f}\kappa_{5b}x_5 - \nu_{5b}\kappa_{5f}x_7}{\kappa_{5f}\kappa_{5b} + \kappa_{5b}x_5 + \kappa_{5f}x_7} - \frac{\nu_6 x_5}{x_5 + \kappa_6} = 0, \\
\text{(b)} \quad &\frac{\nu_{5f}\kappa_{5b}x_5 - \nu_{5b}\kappa_{5f}x_7}{\kappa_{5f}\kappa_{5b} + \kappa_{5b}x_5 + \kappa_{5f}x_7} - \sigma_4 x_7 = 0,
\end{aligned}
\tag{3.2}
$$

with $\xi_1 = v_4 x_2^* / (x_2^* + \kappa_4)$. From (3.2)(b) we obtain

$$x_5^* = \frac{\kappa_{5f} x_7 [v_{5b} + \sigma_4 (\kappa_{5b} + x_7)]}{\kappa_{5b} (v_{5f} - \sigma_4 x_7)},$$

which depends on x_7 and will be positive if $x_7 < v_{5f} / \sigma_4$. By substituting x_5^* into (3.2)(a), we get

$$b_1 (x_7)^3 + b_2 (x_7)^2 + b_3 (x_7) + b_4 = 0, \tag{3.3}$$

with

$$
\begin{aligned}
b_1 &= -\sigma_4^2 \kappa_{5f}, \\
b_2 &= \kappa_{5b} \sigma_4^2 (\kappa_6 - \kappa_{5f}) - \kappa_{5f} \sigma_4 (v_6 - \xi_1 + v_{5b}), \\
b_3 &= -(v_6 - \xi_1)(v_{5b} \kappa_{5f} + \sigma_4 \kappa_{5b} \kappa_{5f}) - (\xi_1 \sigma_4 \kappa_{5b} \kappa_6 + v_{5f} \sigma_4 \kappa_{5b} \kappa_6), \\
b_4 &= \xi_1 \kappa_6 \kappa_{5b} v_{5f}.
\end{aligned}
$$

Now consider the cubic polynomial

$$C(x_7) = b_1 (x_7)^3 + b_2 (x_7)^2 + b_3 (x_7) + b_4, \tag{3.4}$$

whose roots are given by (3.3). Since $b_1 < 0$ and $b_4 > 0$, equation (3.4) has at least one positive root. The positive root x_7^* of (3.4) should be in the required range, $0 < x_7^* < v_{5f} / \sigma_4$, which we will discuss further. By substituting $x_7 = v_{5f} / \sigma_4$ into equation (3.4), we get

$$C\left(\frac{v_{5f}}{\sigma_4}\right) = (\xi_1 - v_6 - v_{5f})(v_{5b} + \kappa_{5b} \sigma_4 + v_{5f}),$$

with $0 < \xi_1 = v_4 x_2^* / (x_2^* + \kappa_4) < v_4$. Since the maximum inflow at the second branch point should be less than the maximum outflow, $v_4 < v_6 < (v_6 + v_{5f})$, $0 < \xi_1 < v_4 < v_6 < (v_6 + v_{5f})$. Consequently, we get $C(v_{5f} / \sigma_4) < 0$. We also find that $C(0) = b_4 > 0$. Applying the intermediate value theorem, the cubic polynomial in (3.4) has a positive root x_7^* in the required range which leads to a positive x_5^*. Since $0 < \xi_1 < v_6$, we have $b_3 < 0$. Thus, the roots that depend on b_2 are either positive or negative. As reported by Lei et al. [19] and Rizzi et al. [25, 26, 31], the magnitude of the Michaelis constant for enzyme alcohol dehydrogenase (κ_{5f}) is higher than that of enzyme acetaldehyde dehydrogenase (κ_6), and so b_2 is negative. Therefore, only one positive root (equilibrium point) is observed. For $b_2 > 0$, there could be three positive roots in the required range. However, hitherto we have lacked information about this case from experiments.

Next, by solving $\dot{x}_6 = 0$, we have

$$c_1 (x_6)^2 + c_2 (x_6) + c_3 = 0, \tag{3.5}$$

with $c_1 = \sigma_3$, $c_2 = \sigma_3 \kappa_7 + v_7 - \xi_2$, $c_3 = -\xi_2 \kappa_7$, $\xi_2 = v_6 x_5^* / (x_5^* + \kappa_6)$. Since $c_1 > 0$ and $c_3 < 0$, it has only one positive root denoted by x_6^*.

Recall that system (2.4) has only one positive steady state,

$$\mathbf{x}_E = \left[\frac{\tilde{G}}{v_1 - \tilde{G}}, x_2^*, \frac{v_2 x_2^*}{(x_2^* + \kappa_2)\sigma_1}, \frac{1}{\sigma_2}\left(\frac{v_3 x_2^*}{x_2^* + \kappa_3} + \frac{v_7 x_6^*}{x_6^* + \kappa_7} \right), \right.$$
$$\left. \frac{\kappa_{5f} x_7^* [v_{5b} + \sigma_4(\kappa_{5b} + x_7^*)]}{\kappa_{5b}(v_{5f} - \sigma_4 x_7^*)}, x_6^*, x_7^* \right],$$

if it satisfies $\tilde{G} < v_1 < v_i$ $(i = 2, 3, 4)$, $v_4 < v_6 < (v_6 + v_{5f})$, and $\kappa_6 < \kappa_{5f}$. Linearizing system (2.4) using a Jacobian matrix evaluated at the positive equilibrium $\mathbf{x}_E$, we obtain a set of linear systems,

$$\dot{\zeta} = J_1 \zeta + J_2 \zeta_\tau,$$

where $\zeta = (x_1(\tilde{t}), \ldots, x_7(\tilde{t}))$, $\zeta_\tau = (x_1(\tilde{t} - 1), \ldots, x_7(\tilde{t} - 1))$, and $J_1 = \left[\begin{array}{c|c} A & \mathbf{0} \\ \hline C & D \end{array} \right]$ and $J_2 = \left[\begin{array}{c|c} A_d & \mathbf{0} \\ \hline \mathbf{0} & \mathbf{0} \end{array} \right]$ are block matrices with

$$A = \begin{bmatrix} 0 & 0 & 0 \\ 0 & -\sum\limits_{i=2}^{4} \dfrac{v_i \kappa_i}{(x_2^* + \kappa_i)^2} & 0 \\ 0 & \dfrac{v_2 \kappa_2}{(x_2^* + \kappa_2)^2} & -\sigma_1 \end{bmatrix},$$

$$A_d = \begin{bmatrix} -\dfrac{(v_1 - \tilde{G})^2}{v_1} & 0 & 0 \\ \dfrac{(v_1 - \tilde{G})^2}{v_1} & 0 & 0 \\ 0 & 0 & 0 \end{bmatrix},$$

$$C = \begin{bmatrix} 0 & \dfrac{v_3 \kappa_3}{(x_2^* + \kappa_3)^2} & 0 \\ 0 & \dfrac{v_4 \kappa_4}{(x_2^* + \kappa_4)^2} & 0 \\ 0 & 0 & 0 \\ 0 & 0 & 0 \end{bmatrix},$$

$$D = \begin{bmatrix} -\sigma_2 & 0 & \dfrac{v_7 \kappa_7}{(x_6^* + \kappa_7)^2} & 0 \\ 0 & -\Lambda_1 & 0 & \Lambda_2 \\ 0 & \dfrac{v_6 \kappa_6}{(x_5^* + \kappa_6)^2} & -\Lambda_3 & 0 \\ 0 & \Lambda_4 & 0 & -\Lambda_5 \end{bmatrix} = [d_{ij}],$$

where

$$\Lambda_1 = \frac{\nu_6 \kappa_6}{(x_5^* + \kappa_6)^2} + \frac{\kappa_{5f} \kappa_{5b} [\kappa_{5b} \nu_{5f} + x_7^* (\nu_{5f} + \nu_{5b})]}{(\kappa_{5f} \kappa_{5b} + \kappa_{5b} x_5^* + \kappa_{5f} x_7^*)^2},$$

$$\Lambda_2 = \frac{\kappa_{5f} \kappa_{5b} [\kappa_{5f} \nu_{5b} + x_5^* (\nu_{5f} + \nu_{5b})]}{(\kappa_{5f} \kappa_{5b} + \kappa_{5b} x_5^* + \kappa_{5f} x_7^*)^2},$$

$$\Lambda_3 = \frac{\nu_7 \kappa_7}{(x_6^* + \kappa_7)^2} + \sigma_3,$$

$$\Lambda_4 = \frac{\kappa_{5f} \kappa_{5b} [\kappa_{5b} \nu_{5f} + x_7^* (\nu_{5f} + \nu_{5b})]}{(\kappa_{5f} \kappa_{5b} + \kappa_{5b} x_5^* + \kappa_{5f} x_7^*)^2},$$

$$\Lambda_5 = \frac{\kappa_{5f} \kappa_{5b} [\kappa_{5f} \nu_{5b} + x_5^* (\nu_{5f} + \nu_{5b})]}{(\kappa_{5f} \kappa_{5b} + \kappa_{5b} x_5^* + \kappa_{5f} x_7^*)^2} + \sigma_4.$$

The characteristic equation is

$$\det[\lambda I_n - J_1 - J_2 e^{-\lambda}] = \det \left[\begin{array}{c|c} \lambda I_3 - (A + A_d e^{-\lambda}) & \mathbf{0} \\ \hline -C & \lambda I_4 - D \end{array} \right] = 0,$$

where I_n is the $n \times n$ identity matrix. Since A, A_d and D are square matrices (see, for instance Meyer's book [20])

$$\det \left[\begin{array}{c|c} \lambda I_3 - (A + A_d e^{-\lambda}) & \mathbf{0} \\ \hline -C & \lambda I_4 - D \end{array} \right] = \det[\lambda I_3 - A - A_d e^{-\lambda}] \det[\lambda I_4 - D] = 0. \quad (3.6)$$

Equation (3.6) leads to

$$\det[\lambda I_4 - D] = (\lambda + \sigma_2) \Big\{ \lambda + \Big(\frac{\nu_7 \kappa_7}{(x_6^* + \kappa_7)^2} + \sigma_3 \Big) \Big\} (\lambda^2 + \alpha \lambda + \beta) = 0, \quad (3.7)$$

with $\alpha = (d_{32} + d_{42}) + (d_{24} + \sigma_4), \beta = d_{32} d_{24} + (d_{32} + d_{42}) \sigma_4$, or

$$\det[\lambda I_3 - A - A_d e^{-\lambda}] = \Big\{ \lambda + \sum_{i=2}^{4} \frac{\nu_i \kappa_i}{(x_2^* + \kappa_i)^2} \Big\} (\lambda + \sigma_1) \Big\{ \lambda + \frac{(\nu_1 - \tilde{G})^2}{\nu_1} e^{-\lambda} \Big\} = 0. \quad (3.8)$$

Solutions of (3.7) are $\lambda_1 = -\sigma_2, \lambda_2 = -(\{\nu_7 \kappa_7 / (x_6^* + \kappa_7)^2\} + \sigma_3)$, and $\lambda_{3,4}$ are roots of the quadratic polynomial in (3.7). Since α and β are positive, $\lambda_{3,4}$ have negative real parts. Consequently, all solutions of (3.7) have negative real parts. Furthermore, from the first and the second terms of (3.8), we obtain $\lambda_5 = -\sum_{i=2}^{4} \{\nu_i \kappa_i / (x_2^* + \kappa_i)^2\}, \lambda_6 = -\sigma_1$, and from the last term

$$\lambda e^{\lambda} = -\frac{(\nu_1 - \tilde{G})^2}{\nu_1} = a_{11}. \quad (3.9)$$

Equation (3.9) is a transcendental equation which has several solutions, all of which can be expressed in terms of the Lambert function $W(x)$ defined by $W(x) \exp(W(x)) = x$, where x can be a complex number (see [8, 32]). Since $a_{11} < 0$, we have the following three conditions:

$$\begin{cases} \lambda_1 < \lambda_2 < 0 & \text{if } -e^{-1} < a_{11} < 0, \\ \lambda_1 = \lambda_2 = -1 & \text{if } a_{11} = -e^{-1}, \\ \text{no real roots} & \text{if } a_{11} < -e^{-1}. \end{cases} \quad (3.10)$$
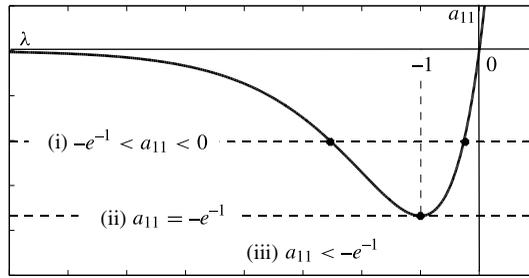
FIGURE 2. The curve for expression (3.10), when $a_{11} < 0$: (i) two different negative solutions; (ii) two equal negative solutions; (iii) complex conjugate solutions.

Expression (3.10) is shown in Figure 2. It indicates that for $-e^{-1} \leq a_{11} < 0$ all the real λ are negative, and it generates a locally asymptotically stable solution for system (2.4). When $a_{11} < -e^{-1}$, oscillatory behaviours may appear in our solutions. To investigate this, suppose that $\lambda = \lambda_R + i\lambda_I$. Substituting this into (3.9) and then separating its real and imaginary parts, we obtain

$$
\begin{aligned}
\text{(a)} \quad & \lambda_R = a_{11}e^{-\lambda_R}\cos\lambda_I, \\
\text{(b)} \quad & \lambda_I = -a_{11}e^{-\lambda_R}\sin\lambda_I.
\end{aligned}
\tag{3.11}
$$

Taking the ratio of both equations, we get

$$
\lambda_R = -\lambda_I \cot\lambda_I.
\tag{3.12}
$$

By substituting (3.12) into (3.11)(b), we find the following relation between a_{11} and λ_I:

$$
\lambda_I = -a_{11}e^{\lambda_I \cot\lambda_I}\sin\lambda_I.
\tag{3.13}
$$

Following the same method as above, the relation between a_{11} and λ_R is given by

$$
\lambda_R = a_{11}e^{-\lambda_R}\cos\left(\sqrt{a_{11}^2 e^{-2\lambda_R} - \lambda_R^2}\right).
\tag{3.14}
$$

The graphs of (3.13) and (3.14) as functions of a_{11} are depicted in Figure 3.

For the special case when $\lambda_R = 0$, we have $\cos\lambda_I = 0$ and $a_{11}\sin\lambda_I = -\lambda_I$ from (3.11). Since $a_{11} < 0$, it implies that

$$
a_{11} = -\lambda_I, \quad \text{for all } \lambda_I = \frac{\pi}{2} + 2n\pi, \quad n \in \mathbb{N}.
\tag{3.15}
$$

After some modifications, the dimensionless form (3.15) becomes

$$
\bar{\tau}_n = \lambda_I(1 - r)^{-2},
$$

where $\bar{\tau}_n = \tau V_1/K_1$ and $r = G/V_1 < 1$, which is the ratio between the rate of glucose supply and the maximum reaction rate of the first enzyme. The $\bar{\tau}_n$ is a critical delay for the appearance of a periodic solution in the neighborhood of a steady state. Here,
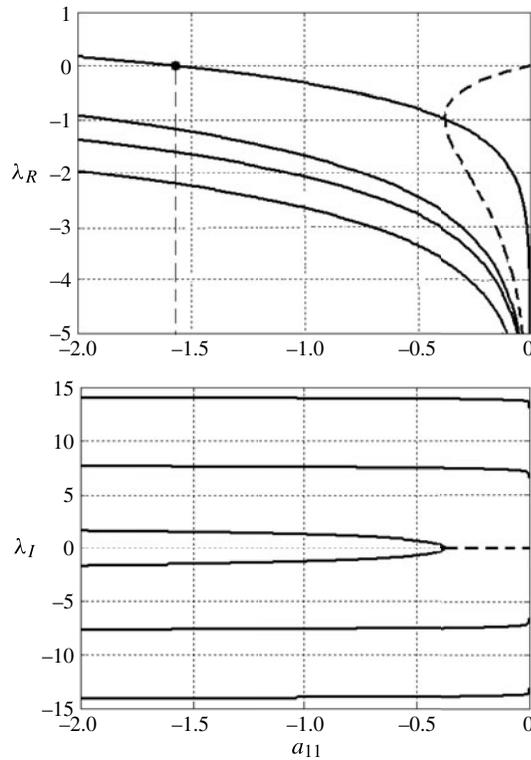
FIGURE 3. Plots of equations (3.13) and (3.14): the real part (top) and the imaginary part (bottom) of λ. Dashed lines denote real solutions ($\lambda_I = 0$) and solid lines denote complex solutions ($\lambda_I \neq 0$). The intersection point at $a_{11} = -(\pi/2) \approx -1.57$ is the point where $\lambda_I \neq 0$, and the sign of λ_R changes from negative to positive.

the stability changes due to the crossing of a conjugate of λ over the imaginary axis, which leads to a Hopf bifurcation (see [10, Chapter 11, Theorem 1.1]).

Although the parameter $\bar{\tau}$ depends only on r, the (real) delay τ actually depends on the three parameters of the first stage reaction: V_1, K_1, and G. Since we may not directly change the kinetic properties of an enzyme without such interventions as adding a molecule effector, that is inhibitor, activator, or inducer [22], the rate of glucose supply is the only parameter that can be controlled from outside. Here changing r means changing the rate of glucose supply in the system for a fixed kinetic parameter of the enzyme. Experimentally, it can be changed by regulating the dilution rate of the growth medium (glucose). By changing the medium flow rate, the growth of the yeast can be easily controlled; for example, Heinrich et al. [12] observed the ethanol production for different medium flow rates. As an illustration, fixing $\lambda_I = \pi/2$, we have a graph of r with respect to $\bar{\tau}$ as shown in Figure 4. Note that for simplicity, we write $\bar{\tau}_0 = \bar{\tau}$. In this figure, we have $\lambda_R = 0$ along the curve, and $\lambda_R \neq 0$ off the curve. Inspecting points off the curve, we have $\lambda_R < 0$ below the curve, indicating a
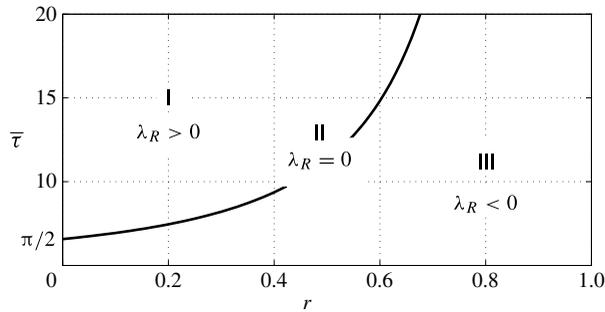
FIGURE 4. Bifurcation diagram for a critical delay $\bar{\tau}$ with respect to r.

stable solution, and $\lambda_R > 0$ above the curve, indicating an unstable solution. These facts allow us to design some strategies or regulations to produce a stable reaction, particularly when delay occurs and the properties of the enzymes are known.

4. Numerical results

We present numerical simulations for three different values of r to validate the analytic results obtained above. Simulations are obtained by using Runge–Kutta methods for delay differential equations (see Shampine and Thompson [29] for details about the method). We use the kinetic parameters shown in Table 1. For our simulations, we take initial concentrations $S_1(t) = 3 \text{ g l}^{-1}$ for all $t \in [-\tau, 0]$, and zero otherwise. We choose $(r, \bar{\tau})$ in the regions I, II, and III in Figure 4, i.e. $r = 0.3, r = 0.4$ and $r = 0.5$, for fixed $\bar{\tau} = 4.4$, respectively.

Figure 5 shows the numerical result for $r = 0.3$. The positive equilibrium solutions (in g l^{-1}) are $S_1^* = 1.04, S_2^* = 4.71, S_3^* = 33.18, S_4^* = 1.35, S_5^* = 0.92, S_6^* = 12.60, S_7^* = 2.66$. The delay leads to an undamped oscillatory behaviour, which leads in turn to the instability of the system. For systems without delay, all solutions tend to approach the equilibrium solution exponentially (see the dashed lines in Figure 5). Moreover, the delay at the first stage affects effectively the oscillations for the first three solutions only.

For $r = 0.4$, we still observe an oscillatory behaviour, but effectively for the first two solutions only (see Figure 6). The solutions are almost periodic with constant amplitudes. For this case, the equilibrium solutions are $S_1^* = 1.62, S_2^* = 7.14, S_3^* = 49.78, S_4^* = 1.35, S_5^* = 0.92, S_6^* = 12.60, S_7^* = 2.66$.

For $r = 0.5$, we obtain equilibrium solutions given by $S_1^* = 2.43, S_2^* = 9.62, S_3^* = 66.38, S_4^* = 1.35, S_5^* = 0.92, S_6^* = 12.60, S_7^* = 2.66$ (see Figure 7). A damped oscillatory behaviour is observed for the first solution only; the amplitude decreases in time. For all cases mentioned above, results from our analyses and simulations are in agreement. An interesting observation comes from the fact that when the kinetic parameters of the first enzyme are known, we can design the value of glucose supply to produce a stable reaction with or without any oscillations.

TABLE 1. The kinetic parameters* reported by Lei et al. [19] and [28].

Par	Value	Unit	Ref.
δ_i	0.38	$[\text{h}^{-1}]$	[19]
K_1	2.43	$[\text{g l}^{-1}]$	[28]
V_1	63.07	$[\text{g g}^{-1} \text{ h}^{-1}]$	[28]
K_2	237.5	$[\text{g l}^{-1}]$	[28]
V_2	648	$[\text{g g}^{-1} \text{ h}^{-1}]$	[28]
K_3	2×10^{-5}	$[\text{g l}^{-1}]$	[19]
V_3	0.501	$[\text{g g}^{-1} \text{ h}^{-1}]$	[19]
K_4	5×10^{-7}	$[\text{g l}^{-1}]$	[19]
V_4	5.81	$[\text{g g}^{-1} \text{ h}^{-1}]$	[19]
K_5^f	0.034	$[\text{g l}^{-1}]$	[19]
V_5^f	2.82	$[\text{g g}^{-1} \text{ h}^{-1}]$	[19]
K_5^b	0.057	$[\text{g l}^{-1}]$	[19]
V_5^b	0.0125	$[\text{g g}^{-1} \text{ h}^{-1}]$	[19]
K_6	2.64×10^{-4}	$[\text{g l}^{-1}]$	[19]
V_6	4.8	$[\text{g g}^{-1} \text{ h}^{-1}]$	[19]
K_7	0.0102	$[\text{g l}^{-1}]$	[19]
V_7	0.0104	$[\text{g g}^{-1} \text{ h}^{-1}]$	[19]

*The units of the kinetic parameters from [28] were converted by using the molecular weight of E_1, E_2 in [28].

To complete our study, we consider the ratio at which the product (ethanol) leaves the cell at the same rate as the reactant (glucose) enters the cell, i.e.

$$Q_{\text{ethanol}} = \frac{\delta_4 S_7}{G}.$$

In Figure 8 (top), we show a steady-state diagram for Q_{ethanol} as a function of G. We observe that there is a certain supply G in which the production of ethanol achieves a minimum production and a maximum production. For small values of G, the ethanol production is low. By increasing G, the production also increases until it achieves a certain supply $\bar{G}$. However, if G increases further from $\bar{G}$, the production decreases. This phenomenon was also observed experimentally by Lei et al. [19] and Postma et al. [23].

We also give the steady-state diagrams of Q_i as a function of G for all products (Figure 8 (bottom)). We observe that ethanol is not the highest product according to the data we used. When ethanol is not the highest product, the metabolic process should
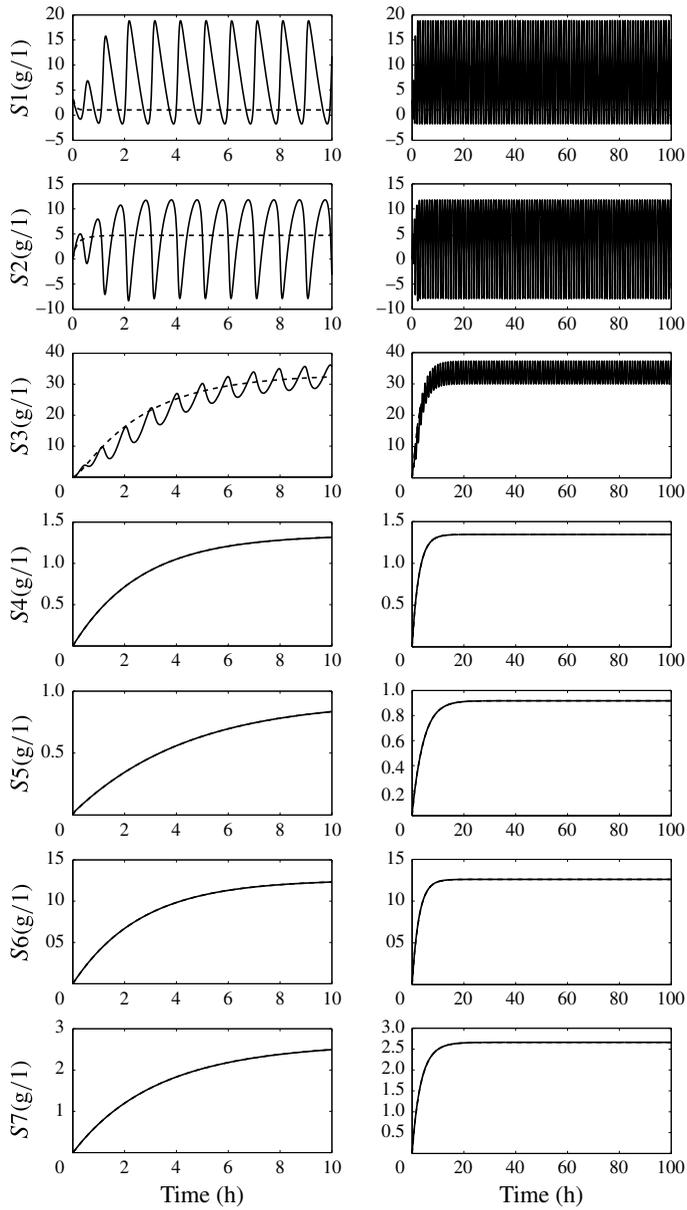
FIGURE 5. Dynamic observation of metabolic system (2.3) with delay (solid line) and nondelay (dashed line) for $r = 0.3$ and $\bar{\tau} = 4.4$ which shows an undamped oscillation: small time (left), large time (right).
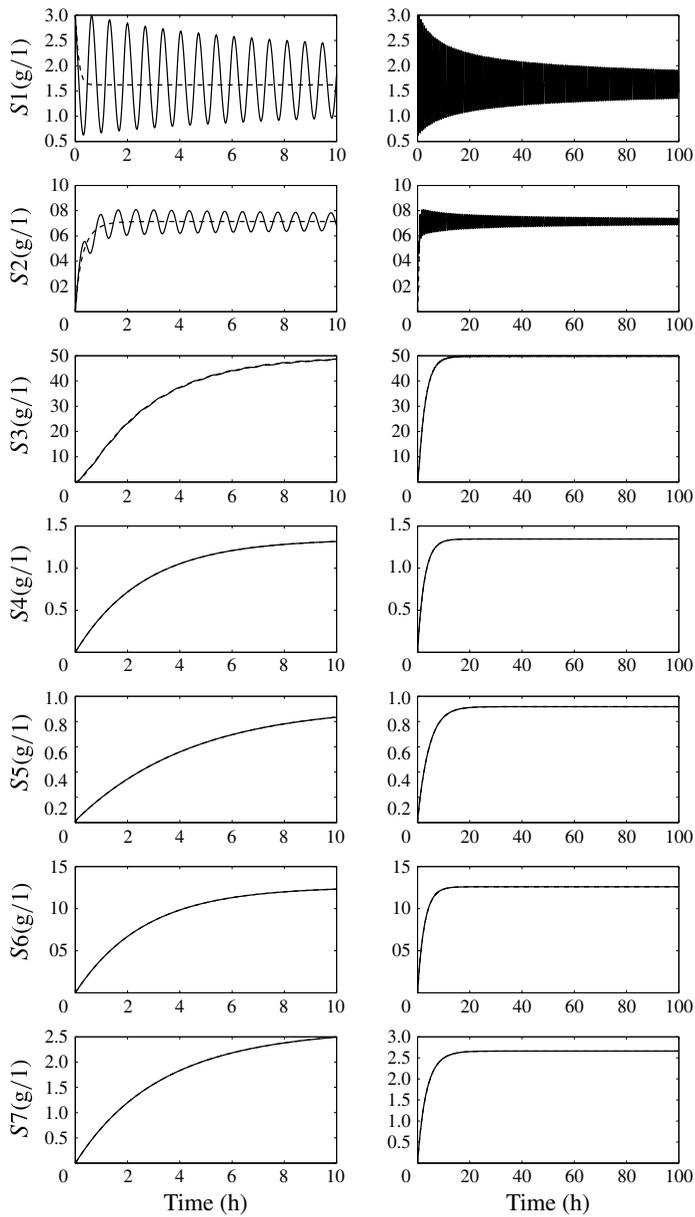
FIGURE 6. Dynamic observation of metabolic system (2.3) with delay (solid line) and nondelay (dashed line) for $r = 0.4$ and $\bar{\tau} = 4.4$ which shows a damped oscillation: small time (left), large time (right side).
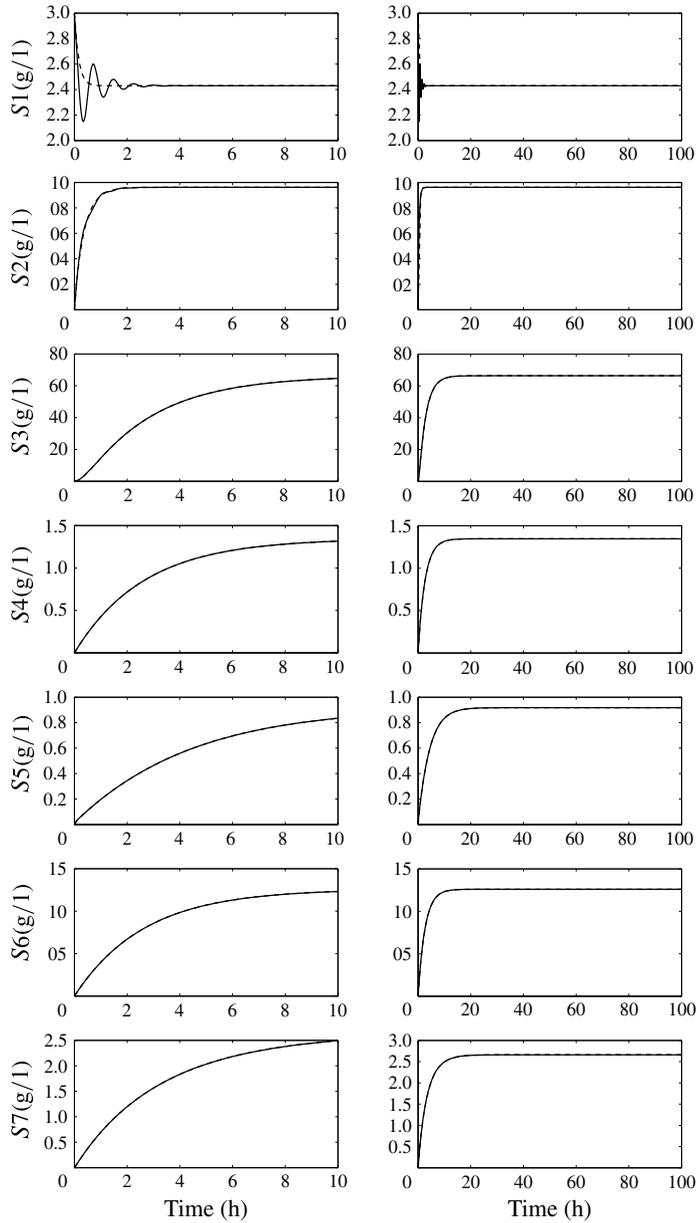
FIGURE 7. Dynamic observation of metabolic system (2.3) with delay (solid line) and nondelay (dashed line) for $r = 0.5$ and $\bar{\tau} = 4.4$ which shows the solution converging exponentially: small time (left), large time (right).
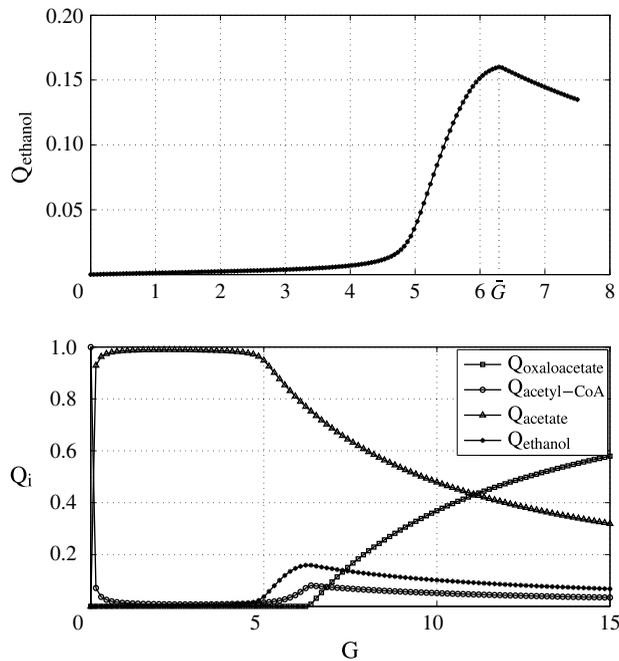
FIGURE 8. Steady-state diagram for Q_{ethanol} as a function of G (top) and Q_i as a function of G for all products (bottom).

be regulated to achieve optimal production of ethanol. This issue can be handled by using a metabolic control analysis, which is the subject of our ongoing research.

5. Conclusions

In this paper, we derived a mathematical model describing the delay effect on the microbial fermentation process. The mathematical formulations presented the transient behaviours of all metabolite concentrations. Analytically, we found a critical delay which depends on the operating parameters of the first stage, i.e. the kinetic parameters of the first enzyme and the rate of constant supply of glucose. This critical delay parameter can be considered as a Hopf bifurcation point that leads to the appearance of oscillatory behaviour in the neighbourhood of the positive equilibrium solution. The existence of the delay in the conversion process directly changed the dynamic behaviour of metabolic system. We found three types of regimes for the solutions: undamped oscillations, damped oscillations, and nonoscillatory behaviour. Numerical results showed that for a fixed kinetic parameter of the enzyme, a rate of glucose supply which can be controlled from the outside, a stable fermentation reaction occurred. Furthermore, there were certain supply values at which ethanol concentration was lowest and highest.

Acknowledgements

Appendix. The Michaelis–Menten kinetic equation for the reversible reaction

Consider the reversible mechanism for the fifth reaction

$$S_5 + E_5 \underset{k_{-1}}{\overset{k_1}{\rightleftharpoons}} E_5 S_5 \underset{k_{-2}}{\overset{k_2}{\rightleftharpoons}} E_5 + S_7$$
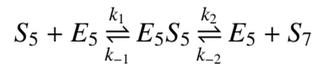
in Figure 1. In both the forward and backward reaction, enzyme E_5 catalyses the conversion of substrate S_5 to produce S_7 at the same constant rate k_i. The dynamics for these reactions are modelled by the following equations:

$$
\begin{aligned}
\text{(a)} \quad & \frac{dS_5}{dt} = k_{-1}E_5S_5 - k_1E_5 \cdot S_5, \\
\text{(b)} \quad & \frac{dE_5S_5}{dt} = -(k_{-1} + k_2)E_5S_5 + (k_1S_5 + k_{-2}S_7)E_5, \\
\text{(c)} \quad & \frac{dE_5}{dt} = (k_{-1} + k_2)E_5S_5 - (k_1S_5 + k_{-2}S_7)E_5, \\
\text{(d)} \quad & \frac{dS_7}{dt} = k_2E_5S_5 - k_{-2}E_5 \cdot S_7.
\end{aligned}
\tag{A.1}
$$

The reaction rate is given by

$$u_5 = -\frac{dS_5}{dt} = \frac{dS_7}{dt}. \tag{A.2}$$

To solve (A.2), some assumptions have been made to simplify the reaction system. Briggs and Haldane [6] assumed that during the reaction, there is a certain time at which a state is reached by the transition state (enzyme complex E_5S_5). It is called *a quasi-steady state* condition [18], which is mathematically described as

$$\frac{dE_5S_5}{dt} = 0. \tag{A.3}$$

Since enzyme is neither produced nor consumed, its total concentration is always constant, $E_5^{\text{total}} = E_5 + E_5S_5$. Consequently,

$$\frac{dE_5}{dt} = 0. \tag{A.4}$$

From (A.1)(b, c), by using (A.3) and (A.4) we obtain

$$E_5 = \frac{(k_{-1} + k_2)E_5^{\text{total}}}{k_1S_5 + k_{-2}S_7 + (k_{-1} + k_2)} \tag{A.5}$$

and

$$E_5 S_5 = \frac{(k_1 S_5 + k_{-2} S_7) E_5^{\text{total}}}{k_1 S_5 + k_{-2} S_7 + (k_{-1} + k_2)}. \tag{A.6}$$

Substitution of (A.5) and (A.6) in (A.2) yields

$$
\begin{aligned}
u_5 &= k_2 E_5 S_5 - k_{-2} E_5 \cdot S_7 \\
&= \frac{k_2 (k_1 S_5 + k_{-2} S_7) E_5^{\text{total}}}{k_1 S_5 + k_{-2} S_7 + (k_{-1} + k_2)} - \frac{k_{-2}(k_{-1} + k_2) E_5^{\text{total}} S_7}{k_1 S_5 + k_{-2} S_7 + (k_{-1} + k_2)}.
\end{aligned} \tag{A.7}
$$

Rewriting this equation in terms of V_5^f, V_5^b, K_5^f, and K_5^b, with $V_5^f = k_2 E_5^{\text{total}}$, $V_5^b = k_{-1} E_5^{\text{total}}$, $K_f = (k_{-1} + k_2)/k_1$, and $K_5^b = (k_{-1} + k_2)/k_{-2}$, we get the reaction rate for the reversible reaction as

$$
\begin{aligned}
u_5 &= \frac{V_5^f S_5 K_5^b - V_5^b S_7 K_5^f}{K_5^f K_5^b + K_5^b S_5 + K_5^f S_7} \\
&= \frac{V_5^f S_5}{K_5^f + S_5 + (K_5^f / K_5^b) S_7} - \frac{V_5^b S_7}{K_5^b + S_7 + (K_5^b / K_5^f) S_5} \\
&= v_5^f - v_5^b.
\end{aligned}
$$

The constants V_5^f and V_5^b are the maximum velocity for the forward and backward reactions, respectively. K_5^f and K_5^b are the Michaelis constants. In both cases, the denominator includes an extra term that shows that S_5 and S_7 are in competition for the same enzyme. Thus each 'substrate' exhibits a competitive inhibition effect on the utilization of the other. For $S_5 = 0$ or $S_7 = 0$, the expression for v_5^f or v_5^b yields the Michaelis–Menten equation for an irreversible reaction.

References

[1] N. Agmon, "Conformational cycle of a single working enzyme", *J. Phys. Chem. B* **104** (2000) 7830–7834; doi:10.1021/jp0012911.

[2] I. C. P. Astudillo and C. A. C. Alzate, "Review: Importance of stability study of continuous systems for ethanol production", *J. Biotechnol.* **151** (2011) 43–55; http://dx.doi.org/10.1016/j.jbiotec.2010.10.073.

[3] S. Benkovic and S. Hammes-Schiffer, "A perspective on enzyme catalysis", *Science* **301** (2003) 1196–1202; http://www.ncbi.nlm.nih.gov/pubmed/12947189.

[4] W. Bennett and T. Steitz, "Glucose-induced conformational change in yeast hexokinase", *Proc. Natl. Acad. Sci. USA* **75** (1978) 4848–4852; http://www.ncbi.nlm.nih.gov/pmc/articles/PMC336218/.

[5] G. Birol, P. Doruker, B. Kardar, Z. I. Onsan and K. Ulgen, "Mathematical description of ethanol fermentation by immobilised *Saccaromyces cerevisiae*", *Process. Biochem.* **7** (1998) 763–771; http://dx.doi.org/10.1016/S0032-9592(98)00047-8.

[6] G. E. Briggs and J. B. Haldane, "A note on the kinetics of enzyme action", *Biochem. J.* **19** (1925) 338–339; http://www.biochemj.org/bj/019/0338/0190338.pdf.

[7] H. S. Christophe, S. E. Jeremy, L. David and O. P. Bernhard, "Combining pathway analysis with flux balance analysis for the comprehensive study of metabolic systems", *Biotechnol. Bioengng* **71** (2001) 286–306; doi: 10.1002/1097-0290(2000)71:43.3.CO;2-I.

[8]   R. M. Corless, G. H. Gonnet, D. E. G. Hare, D. J. Jeffery and D. E. Knuth, "On the Lambert W function", *Adv. Comput. Math.* **5** (1996) 329–359; doi:10.1007/BF02124750.

[9]   E. Eisenmesser, D. Bosco, M. Akke and D. Kern, "Enzyme dynamics during catalysis", *Science* **295** (2002) 1520–1523; doi:10.1126/science.1066176.

[10] J. K. Hale, *Theory of functional differential equations* (Springer, New York, 1977).

[11] R. Heinrich and H. G. Holzhütter, "Efficiency and design of simple metabolic systems", *Biomed. Biochim. Acta* **44** (1985) 959–969; doi:10.1007/BF02460137.

[12] R. Heinrich, H. Holzhütter and S. Schuster, "A theoretical approach to the evolution and structural design of enzymatic networks. Linear enzymatic chains, branched pathways and glycolysis of erythrocytes", *Bull. Math. Biol.* **49** (1987) 539–595; doi:10.1016/S0092-8240(87)90003-6.

[13] R. Heinrich, S. M. Rapoport and T. A. Rapoport, "Metabolic regulation and mathematical models", *Prog. Biophys. Mol. Biol.* **32** (1977) 1–82; http://cmt.hkbu.edu.hk/colloquium/heinrich.pdf.

[14] R. Heinrich and S. Schuster, *The regulation of cellular systems* (Chapman & Hall, New York, 1996).

[15] R. Heinrich and S. Schuster, "The modelling of metabolic systems. Structure, control and optimality", *BioSystems* **47** (1998) 61–77; doi:10.1016/S0303-2647(98)00013-6.

[16] D. Herschlag, "The role of induced fit and conformational changes of enzymes in specificity and catalysis", *Biorg. Chem.* **16** (1988) 62–96; doi:10.1016/0045-2068(88)90038-7.

[17] R. Hinch and S. Schnell, "Mechanism equivalence in enzymesubstrate reactions: distributed differential delay in enzyme kinetics", *J. Math. Chem.* **35** (2004) 253–264; doi: 10.1023/B:JOMC.0000033258.42803.60.

[18] E. Klipp, R. Herwig, A. Kowald, C. Wierling and H. Lehrach, *Systems biology in practice* (Wiley-VCH Verlag, Weinheim, 2005).

[19] F. Lei, M. Rotboll and S. B. Jorgensen, "A biochemically structured model for *Saccaromyces cerevisiae*", *J. Biotechnol.* **88** (2001) 205–221; doi:10.1016/S0168-1656(01)00269-3.

[20] C. D. Meyer, *Matrix analysis and applied linear algebra* (SIAM, Philadelphia, 2000).

[21] J. D. Murray, *Mathematical biology*, 2nd edn (Springer, New York, 1990).

[22] D. L. Nelson and M. M. Cox, *Lehninger: principles of biochemistry*, 4th edn (WH Freeman, Madison, WI, 2005).

[23] E. Postma, C. Verduyn, W. A. Scheffers and J. P. van-Dijken, "Enzymic analysis of the crabtree effect in glucose-limited chemostat cultures of *Saccharomyces cerevisiae*", *Appl. Environ. Microbiol.* **55** (1989) 468–477; http://aem.asm.org/content/55/2/468.short.

[24] J. T. Pronk, H. Yde Steensma and J. P. van-Dijken, "Pyruvat metabolism in *Saccharomyces cerevisiae*", *Yeast* **12** (1996) 1607–1633; http://www.ncbi.nlm.nih.gov/pubmed/9123965.

[25] M. Rizzi, M. Baltes, U. Theobald and M. Reuss, "In vivo analysis of metabolic dynamics in *Saccharomyces cerevisiae*: II. Mathematical model", *Biotechnol. Bioengng* **55** (1997) 592–608; doi:10.1002/(SICI)1097-0290(19970820)55:4<592::AID-BIT2>3.0.CO;2-C.

[26] M. Rizzi, U. Theobald, E. Querfurth, T. Rohrhirsch, M. Bakes and M. Reuss, "In vivo investigations of glucose transport in *Saccharomyces cerevisiae*", *Biotechnol. Bioengng* **49** (1996) 316–327; doi:10.1002/(SICI)1097-0290(19960205)49:3<316::AID-BIT10>3.0.CO;2-C.

[27] M. R. Roussel, "The use of delay differential equations in chemical kinetics", *J. Phys. Chem.* **100** (1996) 8323–8330; doi:10.1021/jp9600672.

[28] I. Schomburg, A. Chang, S. Placzek, C. Shngen, M. Rother, M. Lang, C. Munaretto, S. Ulas, M. Stelzer, A. Grote, M. Scheer and D. Schomburg, "BRENDA in 2013: integrated reactions, kinetic data, enzyme function data, improved disease classification: new options and contents in BRENDA", *Nucleic Acids Res.* **41** (2013) D764–D772; doi:10.1093/nar/gks1049 (database issue).

[29] L. F. Shampine and S. Thompson, "Solving DDEs in MATLAB", *Appl. Numer. Math.* **37** (2001) 441–458; doi:10.1016/S0168-9274(00)00055-6.

[30] B. Sonnleitner and O. Kappeli, "Growth of *Saccharomyces cerevisiae* is controlled by its limited respiratory capacity: formulation and verification of a hypothesis", *Biotechnol. & Bioengng* **28** (1986) 927–937; doi:10.1002/bit.260280620.

[31] U. Theobald, W. Mailinger, M. Baltes, M. Rizzi and M. Reuss, "In vivo analysis of metabolic dynamics in *Saccharomyces cerevisiae*: I. Experimental observations", *Biotechnol. Bioengng* **55** (1997) 305–316; doi:10.1002/(SICI)1097-0290(19970720)55:2<305::AID-BIT8>3.0.CO;2-M.

[32] S. Yi, P. W. Nelson and A. G. Ulsoy, *Time-delay sistems: analysis and control using the Lambert W function* (World Scientific, Singapore, 2010).